

# REMOTE SENSING AND QGIS FOR REGIONAL LANDSLIDE RISK MAPPING: A CASE STUDY OF VARAŽDIN COUNTY, CROATIA

Anja Bek <sup>1\*</sup>, Filip Dodigović <sup>1</sup>, Krešo Ivandić <sup>1</sup>, Jasmin Jug <sup>1</sup>

<sup>1</sup> Faculty of Geotechnical Engineering, University of Zagreb, Hallerova aleja 7, Varaždin 42000, Croatia

\*E-mail of corresponding author: anja.bek@gfv.unizg.hr

**Abstract:** Varaždin County is underlain by Neogene and Quaternary clays and marls that are prone to landslides triggered by intense rainfall. In this study, a landslide risk assessment was carried out for nine municipalities during 2023–2025 using open-source QGIS software and Sentinel-2 imagery. The analysis integrated static factors (slope, aspect, land use) with the dynamic factor NDVI (Normalized Difference Vegetation Index) through Multi-Criteria Decision Analysis (MCDA) and a weighted linear combination. Slope was assigned the highest weight (40%), while NDVI contributed 20%. The results reveal clear spatial contrasts: mountainous municipalities (Donja Voća, Klenovnik, Bednja, Lepoglava, Ivanec) show high to very high landslide risk, whereas lowland municipalities along the Drava River (Cestica, Petrijanec, Maruševac) remain largely stable. Temporal differences are small, with 2023 showing the highest landslide risk and 2024 the lowest. NDVI-driven fluctuations reflect vegetation dynamics but are less influential than topography. Overall, the findings demonstrate the value of open data and free GIS tools for regional hazard mapping. The produced maps provide useful guidance for spatial planning and disaster risk management, while also pointing to the potential of integrating additional datasets in future studies to further improve the robustness of the approach.

**Keywords:** remote sensing; QGIS; landslide risk; slope; aspect; land use; NDVI.

---

Received: 24.10.2025. / Accepted: 10.12.2025.

Published online: 18.12.2025.

---

Original scientific paper

## 1. INTRODUCTION

Landslides are one of the most common natural hazards in Croatia, especially in the northwestern regions such as Međimurska, Krapinsko-zagorska, Varaždinska and Zagrebačka county. These areas are characterised by Neogene and Quaternary clays and marls, which are highly susceptible to slope movements when exposed to intense or long-lasting rainfall. The consequences of landslides include damage to infrastructure, residential areas, and agricultural land, which poses a serious socio-economic problem for local communities (Mihalić Arbanas et al. 2019).

Landslides are generally defined as the downslope movement of rock, debris, or soil under the influence of gravity, typically triggered by external factors such as rainfall, earthquakes, or human activity (Varnes 1978). In line with this general definition, Cruden & Varnes (1996) described landslides as “the movement of a mass of rock, earth, or debris down a slope” and proposed a widely adopted classification system based on the type of material and the nature of movement. This scheme was subsequently refined by Hungr et al. (2014), who emphasized the importance of geological and hydrological conditions in controlling landslide behavior.

At the national level, the first comprehensive assessment of landslide susceptibility in Croatia was presented in the Study: *Procjena podložnosti na klizanje Republike Hrvatske* (Mihalić Arbanas et al. 2019). The study confirmed that northwestern Croatia is among the most landslide-prone regions of the country, with thousands of mapped slope failures and extensive areas predisposed to instability. Catastrophic events triggered by extreme rainfall, such as those during Cyclone Tamara in 2014, further highlighted the vulnerability of this part of Croatia (Mihalić Arbanas et al. 2015).

In northwestern Croatia, a series of scientific studies have applied advanced methods of landslide mapping, monitoring, and modeling. For example, Mihalić Arbanas et al. (2015) provided a comprehensive overview of historical and recent large landslides across the Dinarides and the Pannonian Basin, including northwestern Croatia. More recently, Sinčić et al. (2022) demonstrated the usefulness of high-resolution digital elevation models, land use data, and vegetation indices such as NDVI (for assessing susceptibility in Hrvatsko Zagorje). Their analysis showed that slope angle, lithology, and land cover are the dominant controlling factors, while NDVI proved to be an effective proxy for vegetation cover and its protective role against shallow landslides. The study successfully integrated remote sensing data with GIS-based statistical modeling, resulting in susceptibility maps that highlighted areas of high hazard potential, particularly on steep slopes with reduced vegetation cover. The authors concluded that such an approach provides a reliable basis for regional-scale susceptibility assessment and practical support for local hazard management.

A similar GIS and remote sensing-based methodology was recently applied in Kravarsko, Croatia, where LiDAR-based high-resolution DEMs and land-cover data were combined to develop terrain stability maps for landslide management, without explicit inclusion of lithological parameters (Podolszki & Karlović 2023). This example demonstrates the growing applicability of open-source and data-driven approaches for landslide risk assessment.

Internationally, comparable approaches have been successfully applied. Ayalew and Yamagishi (2005) used GIS-based statistical models for landslide susceptibility mapping in Japan, showing slope angle and topography as key controlling factors. Mersha & Meten (2020) implemented a GIS-based model in northern Ethiopia, combining topographic and environmental predictors with strong predictive performance. Notti et al. (2023) applied a semi-automatic method in northwestern Italy, combining Sentinel-2 NDVI changes with geomorphological filtering through Google Earth Engine to efficiently detect shallow landslides triggered by extreme rainfall. Monopoli et al. (2024) also employed Sentinel-2 change-detection techniques for landslide mapping in Italy, further underlining the utility of multi-temporal NDVI in identifying slope instability.

Varaždin County is located in the northwestern part of Croatia, bordering Međimurje, Krapina-Zagorje, and Koprivnica-Križevci counties, as well as Slovenia to the north. With an area of about 1,262 km<sup>2</sup> and more than 160,000 inhabitants, it is one of the most densely populated regions in the country. The study area includes nine municipalities of Varaždin County which are considered the most susceptible to landslides: Cestica, Petrijanec, Vinica, Maruševac, Donja Voća, Klenovnik, Bednja, Lepoglava, and Ivanec (Figure 1). The total area of the studied municipalities is 495.18 km<sup>2</sup>.

In this county, landslides represent not only a scientific but also a financial and social challenge. Over the past three years, 55 landslides have been remediated on county roads through projects worth around €7 million, financed mainly from EU and national sources, with a smaller share from county funds. Extreme weather conditions in the winter and spring of 2013 further illustrated the region's vulnerability, when more than 900 shallow landslides were (re)activated across northwestern Croatia (Varaždinska županija 2023). Heavy rainfall in May 2023 triggered numerous additional slope failures, leading to the declaration of two natural disasters and causing total damage estimated at €40.95 million, of which about €24.04 million was directly related to landsliding and associated ground deformations, affecting residential buildings, farmland, and road infrastructure (Jug et al. 2024).

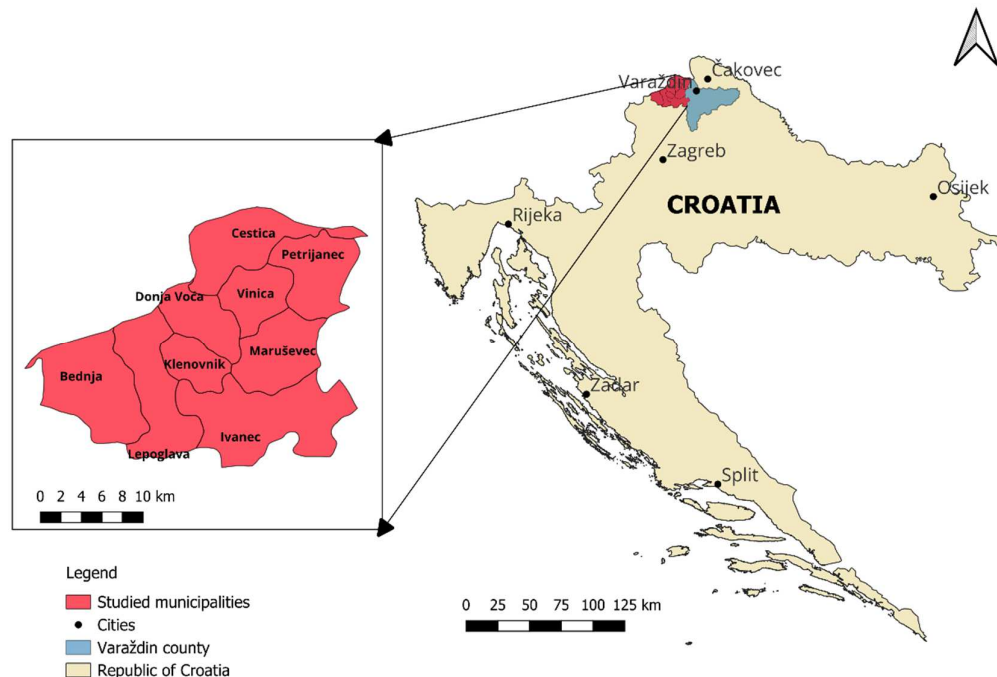


Figure 5. Location of the studied municipalities

The aim of this study is to evaluate landslide risk in nine municipalities of Varaždin County, which are particularly affected by slope instability, by integrating static terrain factors with the Normalized Difference Vegetation Index (NDVI) derived from Sentinel-2 satellite imagery in QGIS. By analysing three consecutive years (2023–2025), the study examines the influence of NDVI changes on slope stability and shows the value of combining remote sensing with open-source GIS tools for regional-scale risk mapping.

## 2. MATERIALS AND METHODS

### 2.1. Used data, their sources and characteristics

In the landslide analysis, the following data were used:

- Digital elevation model (DEM)
- Land use data
- Satellite imagery
- Administrative areas

A digital elevation model (DEM) is a computer-based representation of the Earth's three-dimensional surface, constructed using a raster grid of elevation values. It often refers to both the digital terrain model (DTM), showing the bare-earth surface (without vegetation or built structures), and the digital surface model (DSM), which includes vegetation and buildings. In this study, a DTM was used. DEMs are generated using methods such as InSAR, stereo photogrammetry, LiDAR, and field surveys. They are commonly applied in terrain analysis, hydrology, landslide modeling, GIS, and spatial planning (He et al. 2025).

This study used the Copernicus Digital Elevation Model – GLO-30 (COP-DEM GLO-30), developed under the Copernicus programme and managed by ESA. It is a global elevation model with a spatial resolution of 30 metres, based on data from the TanDEM-X mission. The model represents the “bare-earth” surface. The most recent available and used version of the COP-DEM GLO-30 is Release 2023\_1, published in December 2023. The data were downloaded in GeoTIFF format and comply with international spatial data standards, including the INSPIRE Directive. The DEM is orthorectified and corrected for distortions caused by terrain slopes and sensor noise, ensuring high accuracy and reliability in spatial analyses (ESA 2020).

DEM is used to derive two key topographic factors in landslide analysis: slope and aspect. These factors significantly influence terrain stability and are commonly used in spatial landslide hazard modeling.

Land use data were obtained from the CLCplus Backbone 2023 dataset provided by the Copernicus Land Monitoring Service. This product offers a 10 m resolution raster depicting dominant land cover and land use classes across Europe. Using Sentinel-2 time-series imagery and decision-tree algorithms, a total of eleven thematic categories (Figure 2) are classified annually. The dataset is widely used in environmental monitoring, spatial planning, landslide analysis, and climate policy implementation, with a reported thematic accuracy exceeding 90% (Need 2021; Copernicus Land Monitoring service 2023).

Land use data were provided as a preprocessed raster, in which the original eleven categories were subsequently reclassified into five landslide stability categories.

Slope and exposure, calculated from the digital elevation model (DEM), together with land use data, represent static factors in the landslide analysis, as they remain constant for all three observed years (2023, 2024, and 2025), given that the latest available data is from 2023.

Remote sensing satellite imagery refers to the acquisition of Earth surface data by capturing reflected electromagnetic radiation using satellite sensors (e.g., Sentinel-2, Landsat, PlanetScope). The resulting image is a structured raster in which each pixel represents the amount of reflected radiation from the land surface. These images consist of multi-band raster data, with each spectral band capturing reflectance within a specific wavelength range. Sentinel-2 imagery, for example, comprises thirteen spectral bands designed for detailed monitoring of land and vegetation. Satellite imagery is widely used for mapping land use and land cover changes, assessing soil and vegetation characteristics, modeling natural disaster risks (such as landslides), and monitoring environmental processes through geospatial analysis (Issaoui et al. 2024; European Space Agency 2025).

For the calculation of the NDVI (Normalized Difference Vegetation Index), Sentinel-2 satellite images with a spatial resolution of 10 m were used, sourced from the Copernicus Data Space Ecosystem (Copernicus Data Space Ecosystem). Satellite imagery from June 19, 2023; June 18, 2024; and June 10, 2025 was selected for the respective analysis years.

NDVI, derived from satellite imagery, represents a dynamic factor, as its values vary depending on the year of observation. The final outcome of the analysis will rely solely on changes in NDVI across the observed years.

The data used to calculate landslide conditioning factors, derived from the digital elevation model (DEM) and land use information, were obtained as raster files in .tiff format and subsequently processed. Visualization of all rasters after classification was performed by applying discrete values for interpolation and selecting different color displays that best represent individual values or categories. All analyses were conducted using the official coordinate reference system of the Republic of Croatia – EPSG:3765 (HTRS / Croatia TM) (Lapaine 2024).

Since all the downloaded data used for the landslide analysis cover a broader area than the actual study region, administrative boundaries of the Republic of Croatia (vector data) were obtained from the DIVA-GIS platform (Diva-GIS). The HRV\_adm2 layer, provided in .shp format and containing divisions by municipalities and cities, was used to extract only the areas of the municipalities included in the study using the attribute table.

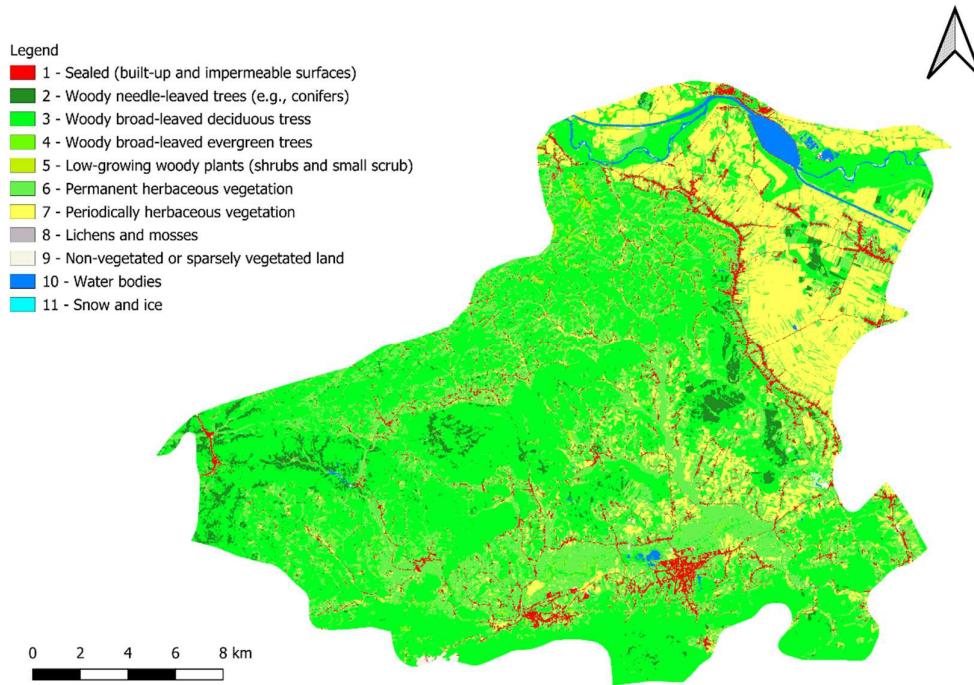


Figure 6. Land use data for studied municipalities classified into 11 categories (Issaoui et al. 2024)

## 2.2. Slope

The slope function in QGIS calculates terrain steepness based on a digital elevation model (DEM). Local slope is estimated for each pixel using elevation differences within a 3×3 pixel window. Partial derivatives in the x and y directions are computed from the elevation differences between neighboring cells, and slope is then derived using the Pythagorean theorem (**Equation 1**) (Esri 2024).

$$\tan \alpha = \sqrt{\left(\frac{\partial z}{\partial x}\right)^2 + \left(\frac{\partial z}{\partial y}\right)^2} \quad (1)$$

Where  $\frac{\partial z}{\partial x}$  and  $\frac{\partial z}{\partial y}$  are the elevation changes in the x- and y-directions (east–west and north–south), and  $\alpha$  is the slope angle calculated as the arctangent of the resultant gradient of these values (Esri 2024).

The result is a raster layer with values expressed in degrees or percent, where lower values indicate flatter terrain and higher values steeper slopes. The tool is accessed through the Processing Toolbox (Raster → Analysis → Slope), where the DEM is selected and the output format is defined. In this study, slope was used in degrees (ranging from 0° to 90°) (Esri 2024; Xiong et al. 2022).

Although there is no universal division and standard, and it often depends on the terrain conditions and the author's judgment, slope angle classifications of 0–5°, 5–15°, 15–25°, 25–35° and >35° or very similar values are widely used in landslide analysis (Klimeš and Rios Escobar 2010; Tzampoglou et al. 2025; Rana et al. 2025). Gazibara et al. (2023) in their analysis of the Zagreb landslide mention slope as a determining factor in modeling landslide occurrence, but they do not use an explicit interval division. Therefore, this paper uses a similar slope classification supported by recent landslide research (Tzampoglou et al. 2025; Rana et al. 2025). The classification of the slide test slope and the description of the terrain are based on expert interpretation, using the thresholds from Klimeš et al. (2010). and adapted for the needs of local geomorphological analysis (**Table 1**). The classification of landslide stability and division into categories is based on the author's observation and professional experience.

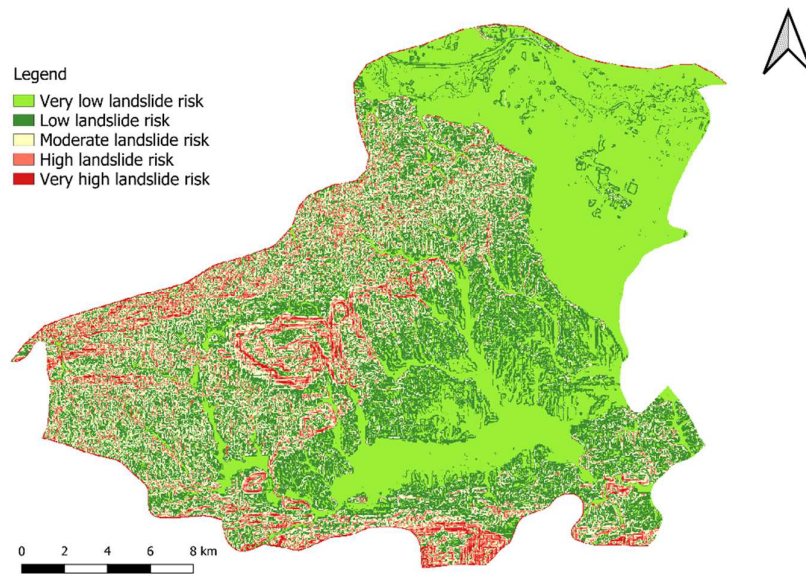
Although slope categories >35° are often associated with a high risk of landslide occurrence, it should be noted that in geological contexts dominated by hard, intact rocks, such slopes can remain stable in the author's experience. Groundwater can also affect stability, but is not considered in this paper.

For easier later addition of the raster and calculation of the comprehensive risk of landslides, the Slope risk factor (and other factors - aspect, land use and NDVI) are classified into five categories using the Raster calculator function as shown in **Table 1**.

**Table 5.** Slope category, terrain description and corresponding landslide stability categories

Slope of the sliding surface (Klimeš et al. 2010)	Terrain description	Risk category	Category
0–5°	Flat terrain	Very low landslide risk	1
5–15°	Gently undulating terrain	Low landslide risk	2
15–25°	Undulating to moderately steep terrain	Moderate landslide risk	3
25–35°	Steep terrain	High landslide risk	4
>35°	Very steep terrain	Very high landslide risk	5

**Figure 3** shows the slope risk factor map classified into five categories based on landslide risk for the studied municipalities.

**Figure 7.** Slope risk factor map

### 2.3. Aspect

The aspect function indicates the orientation of a slope (expressed in degrees 0–360°), in other words, the cardinal direction toward which the slope faces most steeply downhill. Flat areas (without slope) are assigned a value of 0 and have no defined aspect. Slope orientation influences insolation, moisture, and vegetation, which are of particular importance for slope stability. Similar to the slope function, the aspect function is accessed through the Processing Toolbox (Raster → Analysis → Aspect).

Horn (1981) defines aspect as the direction of maximum slope for an individual DEM cell, calculated on the basis of partial derivatives of elevation in the x and y directions, derived from a 3×3 neighborhood of raster cells, according to the following equation (Horn 1981):

$$\alpha = \arctan 2 \left( \frac{\partial z}{\partial x}, \frac{\partial z}{\partial y} \right) \quad (2)$$

where  $\alpha$  is the slope orientation (in this study expressed in degrees),  $\frac{\partial z}{\partial x}$  is the partial derivative in the x-direction (the change in elevation in the east–west direction) and  $\frac{\partial z}{\partial y}$  is the partial derivative in the y-direction (the change in elevation in the north–south direction).

The result of the aspect function is a raster in degrees from 0 to 360, which indicates the cardinal directions. The classification of directions according to degrees is defined by specific intervals (**Table 2**), which are often applied in landslide research in QGIS (Swain et al. 2024; Liu et al. 2024). The description of insolation and moisture conditions associated with slope aspect in a temperate climate (e.g., north-facing slopes being cooler and moister, south-facing slopes warmer and drier) is based on general geomorphological interpretation supported by recent studies (Wang et al. 2025; Zhu et al. 2025). In this study, the insolation and moisture conditions of the intermediate directions were also taken into account, as they are considered transitional.

**Figure 4** and **Table 2** shows the risk factor map of aspect, classified into five categories with corresponding descriptions using the Raster calculator function for the studied municipalities.

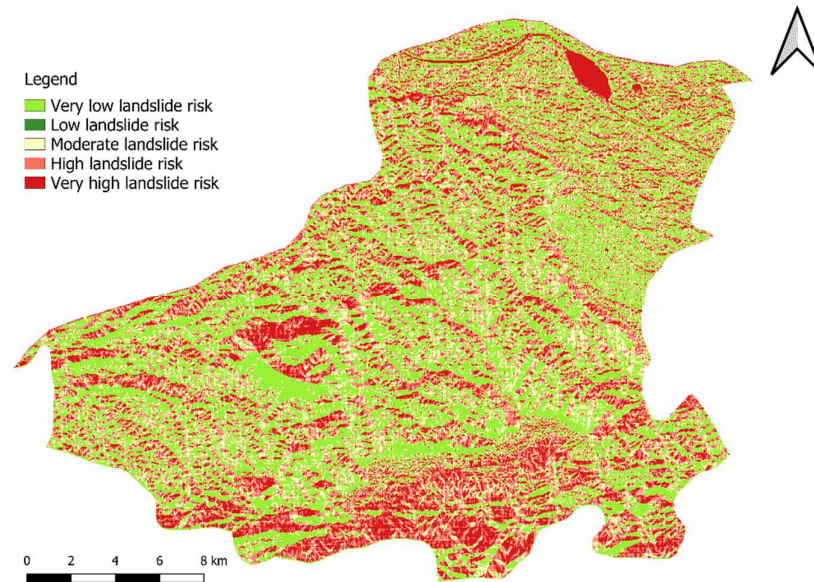


**Figure 8.** Aspect risk factor map

**Table 6.** Description of the aspect raster with classification into five categories

Degrees (°) (Swain et al. 2024; Liu et al. 2024)	Cardinal direction (Swain et al. 2024; Liu et al. 2024)	Insolation and moisture	Category	Risk category
337.5 – 360 and 0 – 22.5	North	Most humid, least insolated	5	Very high landslide risk
22.5 – 67.5	Northeast	Humid, partially insolated	4	High landslide risk
67.5 – 112.5	East	Moderately humid, balance of sun and shade	3	Moderate landslide risk
112.5 – 202.5	Southeast – South	Dry slopes	1	Very low landslide risk
202.5 – 247.5	Southwest	Dry slopes (possible temporary water retention)	2	Low landslide risk
247.5 – 292.5	West	Moderately humid, balance of sun and shade	3	Moderate landslide risk
292.5 – 337.5	Northwest	Humid, partially insolated	4	High landslide risk

## 2.4. Land use

Land use raster refers to human activities, management practices, and socioeconomic purposes assigned to land. It reflects how people interact with, manage, and modify the land surface for purposes such as agriculture, urban development, forestry, or recreation. Land use is shaped not only by visible cover, but also by institutional, policy, and functional considerations (Copernicus Land Monitoring Service 2025).

As mentioned earlier, the land use raster is a pre-prepared raster divided into eleven classes (not calculated based on DEM such as slope and aspect). The reclassification of land use classes into five categories of landslide risk was carried out according to the guidelines of recent and slightly older research (Table 3) (Swain et al. 2024; Corominas et al. 2014; Reichenbach et al. 2018; Putra et al. 2025). Forest areas are classified in the very low category, shrubs and permanent vegetation in the low category, occasional vegetation and lichens in the moderate category, sparse vegetation in the high category, while artificial surfaces (built-up areas) are in the very high risk category. Water and ice surfaces are excluded from the analysis or assigned to the very low category, as in this paper. Reclassification was carried out using a raster calculator. Figure 5 shows a land use risk raster reclassified into five categories according to landslide risk for the studied municipalities (Corominas et al. 2014; Reichenbach et al. 2018; Putra et al. 2025).

**Table 7.** Description of the land use raster with reclassification into 5 categories (Swain et al. 2024; Corominas et al. 2014; Reichenbach et al. 2018; Putra et al. 2025)

Original class	New category	Risk category	Description of landslide risk
2, 3, 4 – Forests (coniferous, deciduous, evergreen)	1	Very low landslide risk	Forests stabilize soil, roots bind the substrate, surface runoff is reduced.
10 – Water bodies 11 – Snow and ice	1 or no data	Very low landslide risk	Landslides do not develop within water/ice, only at edges – usually classified as very low or excluded.
5, 6 – Shrubs, permanent vegetation	2	Low landslide risk	Vegetation stabilizes, but less effectively than forests; risk is slightly higher.
7, 8 – Temporary vegetation, lichens, mosses	3	Moderate landslide risk	Temporary cover means weaker soil retention and variable moisture conditions.
9 – Sparse or bare vegetation	4	High landslide risk	Lack of cover increases erosion and surface runoff - high instability.
1 – Artificial surfaces (settlements, roads, concrete)	5	Very high landslide risk	Human activities (construction, slope cutting, soil removal) significantly increase risk.

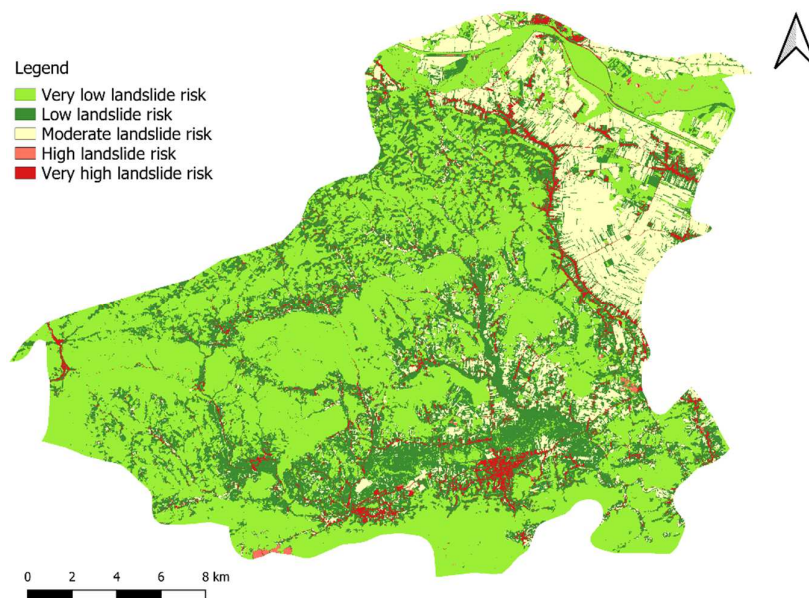


**Figure 9.** Land use risk factor map

## 2.5. NDVI index

The Normalized Difference Vegetation Index (NDVI) is a key remote sensing tool that enables scientists and experts to monitor vegetation dynamics (density and growth), classify land use, predict crop yields, monitor vegetation responses to climate change, and biomass production using satellite images. It is calculated using the Raster calculator function based on the following equation (O'Donohue 2023):

$$NDVI = \frac{NIR - RED}{NIR + RED} \quad (3)$$

where NIR (Band 8 in Sentinel-2 satellite images) represents near-infrared light that is strongly reflected by vegetation, and RED (Band 4 in Sentinel-2 satellite images) represents visible red light that is absorbed by vegetation. The resulting value can range from -1 to 1, with higher values indicating healthier and denser vegetation (O'Donohue 2023; Zhao et al. 2024).

The NDVI index was calculated based on satellite images taken on the following dates: June 19, 2023, June 18, 2025, and June 10, 2025. After calculating the NDVI index, the rasters were classified into five categories of landslide risk according to the NDVI value ranges and vegetation description (Table 4). The NDVI ranges and vegetation descriptions were taken from relevant articles with minor additions (Wen and Teo 2022; Plank et al. 2016), while the stability categories were determined according to the author's experience and their interpretation of the relationship between vegetation and terrain susceptibility to landslides.

Figure 6 shows the NDVI index classified into five categories according to the risk of landslide occurrence for 2023, 2024, and 2025.

**Table 8.** Description of the properties of the NDVI rasters divided into five categories

NDVI Range (Wen and Teo 2022; Plank et al. 2016)	Vegetation Description (Wen and Teo 2022; Plank et al. 2016)	Category	Risk Category
> 0.60	Very dense vegetation – dense forest, stable soil	1	Very low landslide risk
(0.40 – 0.60]	Dense vegetation – semi-forest, forest edge	2	Low landslide risk
(0.25 – 0.40]	Moderate vegetation – shrubs, bush	3	Moderate landslide risk
(0.10 – 0.25]	Very sparse vegetation – degraded vegetation, dry	4	High landslide risk
< =0.10	No vegetation – bare soil, rocks, water, built-up area	5	Very high landslide risk

## 2.6. Component formula for calculating landslide risk

For the overall assessment of landslide risk, the Multi-Criteria Decision Analysis (MCDA) method was applied using the Weighted Linear Combination (WLC) approach (Malczewski 1999). Four risk factors were included in the analysis: slope, aspect, NDVI, and land use, which are most frequently highlighted in various studies as relevant to slope stability (Podolszki 2023; Guzzetti et al 1999; Pourghasemi et al 2012).

Weights were assigned according to the relative importance of each factor in the landslide formation process. Slope was assigned the highest weight (0.40), as it is one of the key factors in landslide occurrence. Aspect was assigned a medium weight (0.25) due to the influence of insolation and moisture. NDVI was given a weight of 0.20, since vegetation cover reduces erosion and instability, while land use had the lowest weight (0.15).

It is important to emphasize that the specific weight values were determined through a combination of expert judgment, methodological decisions, and guidelines from the literature (Podolszki 2023; Malczewski 1999; Guzzetti et al 1999; Pourghasemi et al 2012) and were not taken from a single specific study. The composite equation using the crude risk index for regional spatial analysis for all three observed years is as follows:

$$Total\ risk = (Slope \cdot 0.40) + (Aspect \cdot 0.25) + (NDVI \cdot 0.2) + (Land\ use \cdot 0.15) \quad (4)$$

The result of this equation is a composite risk raster with values ranging from 1 to 4.35. In order to obtain a raster with five risk categories, the obtained values were divided into categories (Table 5). In recent studies on landslide risk and susceptibility, a classification into five categories with irregular intervals is often used. This division method distinguishes areas of different risk better than equal intervals, and is flexible enough to adapt to the distribution of data and specific terrain characteristics. This division – from very low to very high risk – has been shown to facilitate the interpretation of results and their practical application in spatial planning (He et al. 2025; Zhang et al. 2025; Fuad et al. 2024).

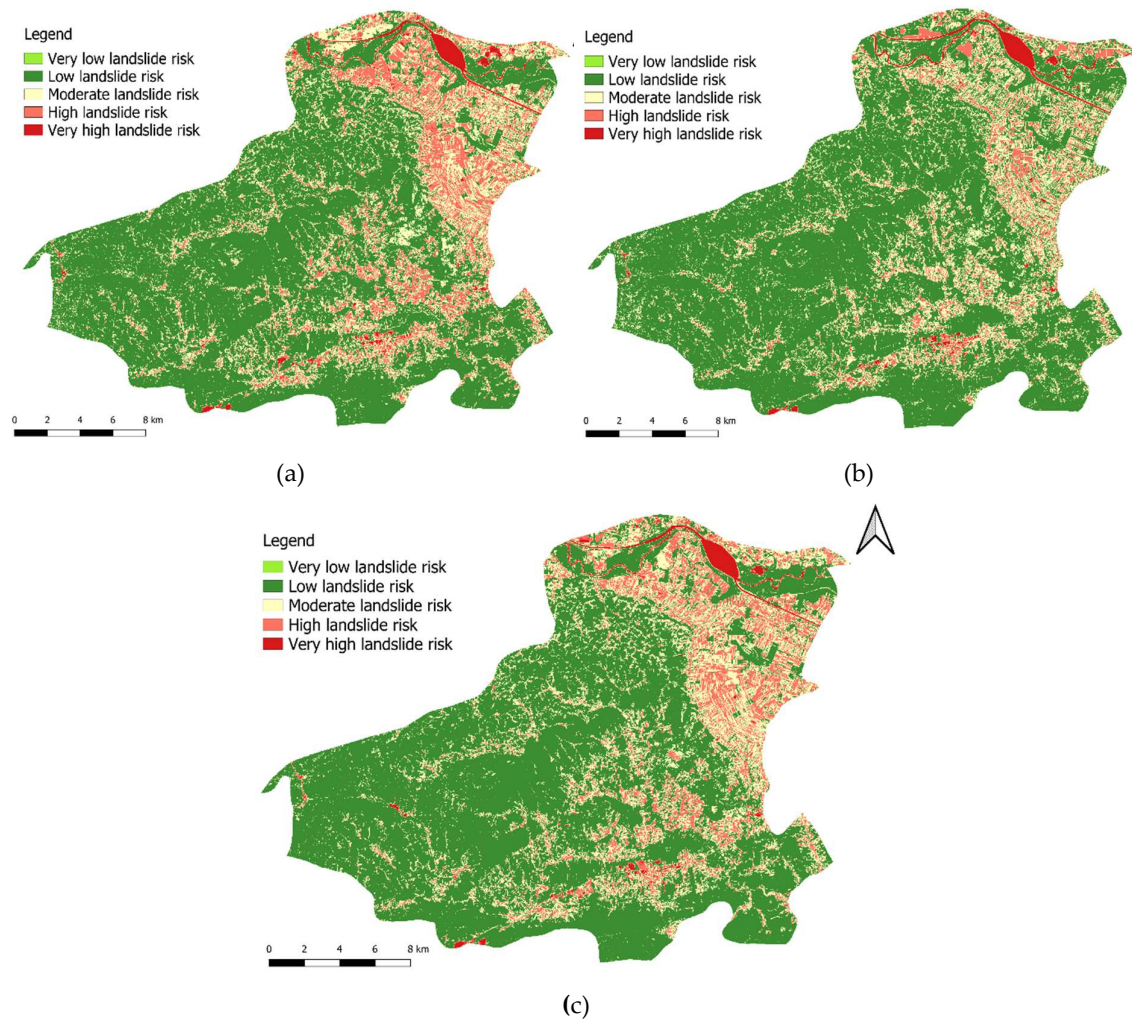


Figure 10. NDVI risk factor map: (a) June 19, 2023; (b) June 18, 2024; (c) June 10, 2025

Table 9. Division of the composite landslide risk raster according to the interval value into five categories (He et al. 2025; Zhang et al. 2025; Fuad et al. 2024)

Interval	Category	Risk category
(1 - 1.5]	1	Very low landslide risk
(1.5 - 2.2]	2	Low landslide risk
(2.2 – 2.9]	3	Moderate landslide risk
(2.9 – 3.6]	4	High landslide risk
(3.6 – 4.35]	5	Very high landslide risk

### 3. RESULTS

#### 3.1. Landslide risk maps

After the analyses were conducted, landslide risk maps were obtained for the studied municipalities, which include all four risk factors (slope, aspect, NDVI and land use). **Figure 7** shows the landslide risk map for 2023, **Figure 8** for 2024, and **Figure 9** shows the landslide risk map for 2025. Five categories of landslide risk are shown in different colours. The lowest category (1) is marked in green and represents a very low risk of landslide. The highest category (5) is marked in red and represents a very high risk of landslide. Transitional categories are

defined between categories 1 and 5. Differences in the risk of landslide occurrence by year are minor because all changes result from the difference in the NDVI index, which is assigned a weight of 0.20 (20% contribution in the map display). Other factors (slope, aspect and land use) are the same for all analyzed years because the data is not updated annually, and the latest available data is from 2023.

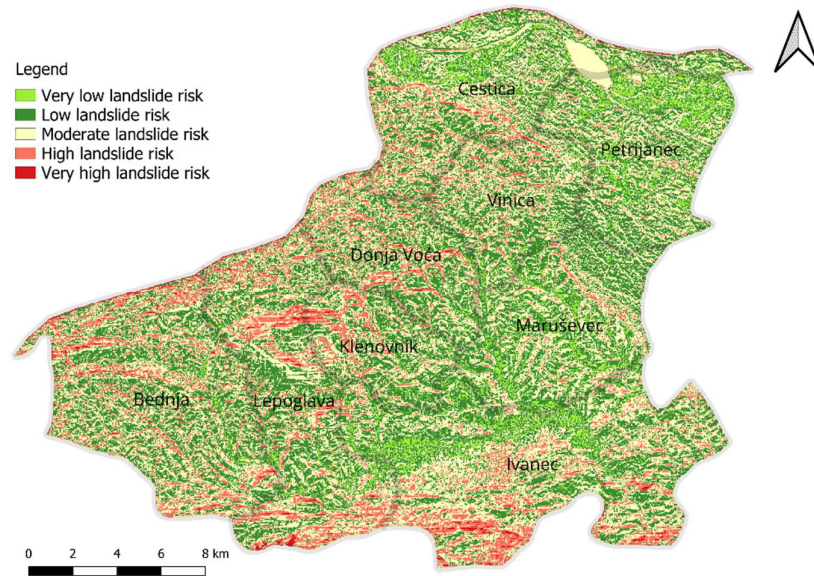


**Figure 11.** Landslide risk map for 2023

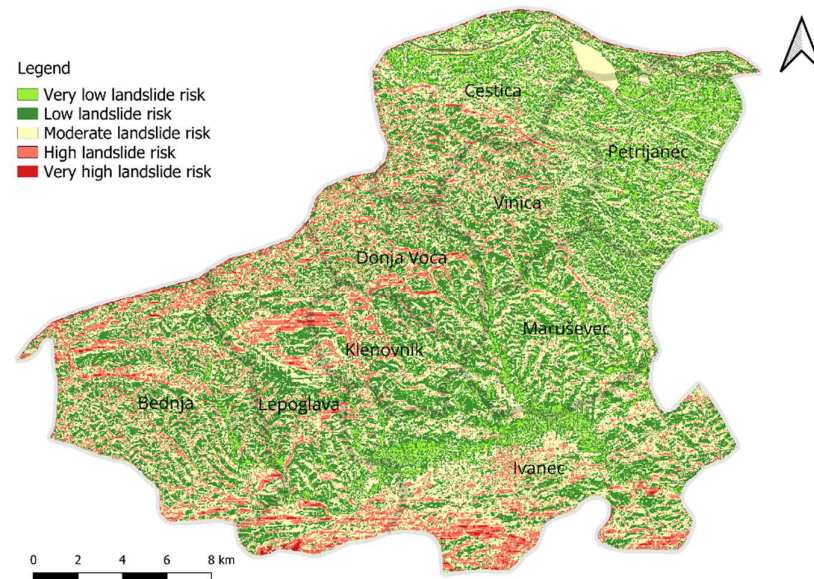


**Figure 12.** Landslide risk map for 2024

As can be seen from the attached maps, the highest risk of landslides (very high and high) is in the municipalities bordering Slovenia (Donja Voća, Klenovnik, Bednja and Lepoglava) and the municipality of Ivanec, especially in the area of mountain Ivanščica. The lowest risk of landslides is in the areas at the foot of mountain Ivanščica (Ivanec municipality) and the municipalities of Cestica, Petrijanec and Maruševec, where the influence of the Drava river is possible, so lowland areas predominate.

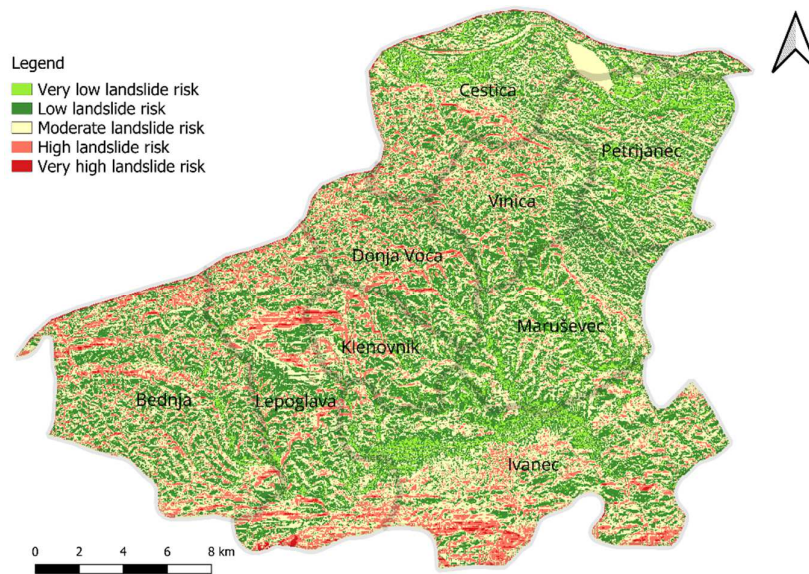


Figure 13. Landslide risk map for 2025

**Table 6** shows the areas and shares of areas for all five categories according to the analyzed years. The year 2024 has the highest area in category 1 (very low landslide risk) with 39.90 km<sup>2</sup> (8.06%). This is followed by 2025 with 32.67 km<sup>2</sup> (6.60%), and 2023 has the lowest area in category 1 at around 31.12 km<sup>2</sup> (6.28%).

The second category (low risk of landslides) has the largest area in 2025 (193.77 km<sup>2</sup>, i.e. 39.13%), and the smallest in 2024 with 191.21 km<sup>2</sup> (38.61%). The areas of the second category are very similar; the difference is only about 0.5%.

The largest area with moderate landslide risk (category 3) belongs to 2023 with 197.25 km<sup>2</sup> (39.83%), and the smallest is in 2024 with an area of about 193.52 km<sup>2</sup> (39.08%).

Category 4 (high risk of landslides) occupies the largest area in 2023 (69.59 km<sup>2</sup>, 14.05%), and the smallest area in 2024 with 65.97 km<sup>2</sup> (13.32%).

The highest risk of landslides (Category 5) is in 2023 (4.66 km<sup>2</sup>, 0.94%). 2025 has the smallest area (4.55 km<sup>2</sup>, 0.92%) in the category of very high risk of landslides.

Based on the analysis and comparison of areas, it can be determined that the highest risk of a landslide occurring is in 2023, and the lowest risk of a landslide occurring is in 2024.

**Table 10.** Area and percentage by soil stability categories for 2023, 2024 and 2025

Risk Category	2023 [km <sup>2</sup> ]	2023 [%]	2024 [km <sup>2</sup> ]	2024 [%]	2025 [km <sup>2</sup> ]	2025 [%]
1-Very low landslide risk	31.12	6.28	39.90	8.06	32.67	6.60
2-Low landslide risk	192.56	38.89	191.21	38.61	193.77	39.13
3-Moderate landslide risk	197.25	39.83	193.52	39.08	196.23	39.63
4-High landslide risk	69.59	14.05	65.97	13.32	67.96	13.72
5-Very high landslide risk	4.66	0.94	4.58	0.93	4.55	0.92

### 3.2. Landslide risk maps

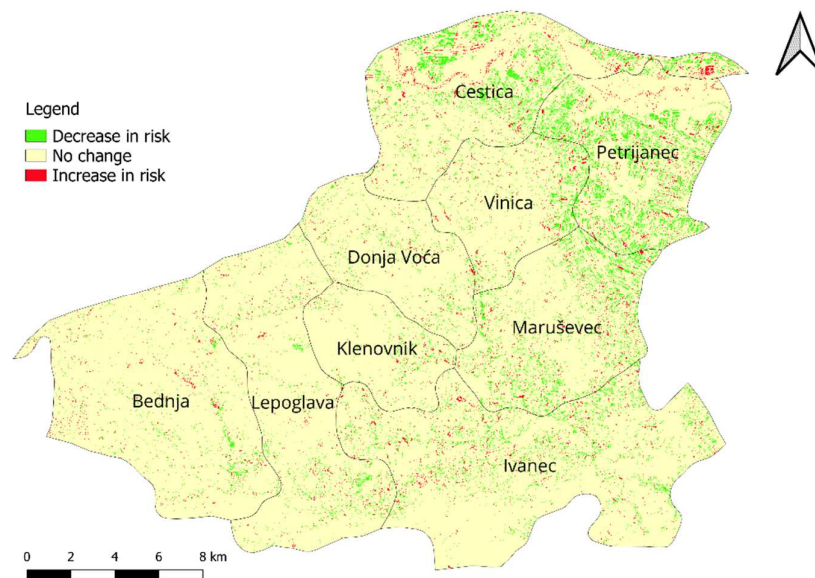
Landslide risk change maps were produced by subtracting the landslide risk map of the reference year from the map of the analyzed year. In this way, values in the range from -1 to 1 were obtained. The values were then classified into three categories: decrease in risk, no change, and increase in risk. Only these three categories were defined because there were no data in the ranges from -0.6 to -0.2 and from 0.2 to 0.6 (**Table 7**).

Since the difference was calculated as (analyzed year – reference year), positive values indicate an increase in landslide risk in the analyzed year compared to the reference year, while negative values indicate a decrease in risk.

**Table 11.** Landslide risk categories based on risk difference values

Category	Value range	Risk category
1	-1.00 to -0.20	Decrease in risk
2	-0.20 to 0.20	No change
3	0.20 to 1.00	Increase in risk

**Figure 10** indicates the landslide risk map in 2024 (the analyzed year) compared to 2023 (the reference year). From the **Figures 10, 11** and **12** and **Table 8** it is clear that the highest area of the studied area is without change (risk) of more than 90 % (as in the other analyzed risk maps). The year 2024 shows a greater decrease in the risk of landslide occurrence (about 28.75 m<sup>2</sup>, 5.81%) compared to 2023. An area of 8.79 km<sup>2</sup> (1.76%) is prone to an increase in the risk of landslide occurrence. The most pronounced decrease in the risk of landslides is in the area of the municipalities of Cestica and Petrijanec, and in the peripheral parts of these municipalities with the municipalities of Vinica and Maruševec.

**Figure 14.** Landslide risk map in 2024 compared to 2023

A comparison of the risk of landslides in 2025 compared to 2024 (**Figure 11**) shows that in 2025, the risk of landslides increased in more areas than it decreased, by approximately 25.01 km<sup>2</sup>, or 5.05% (**Table 8**). The risk reduction covers an area of 11.20 km<sup>2</sup> (2.26%). The largest increase in risk in 2025 was recorded in the municipalities of Cestica, Petrijanec and Maruševec.

The last risk map, comparing the risk of landslides in 2025 compared to 2023 (**Figure 12**), indicates that a larger part of the studied landslide area has a decrease in the risk of landslides in 2025 (17.44 km<sup>2</sup>, i.e. 3.52%). An increase in risk was recorded on 11.25 km<sup>2</sup> (2.27%) of the area.

The attached landslide risk maps confirm that the highest risk and risk of landslides is in 2023 because, compared to 2024 and 2025, the largest part of the area corresponds to category 3 (increased risk). Also, the results of the risk maps confirm that the lowest risk of landslides (the smallest area in the increased risk zone) is in 2024, as determined by the landslide risk maps.

The analyzed risk maps indicate that 2025 represents a transitional state, positioned between 2023, which shows the highest increase in landslide risk, and 2024, which reflects the lowest increase, i.e. the most significant reduction in risk.

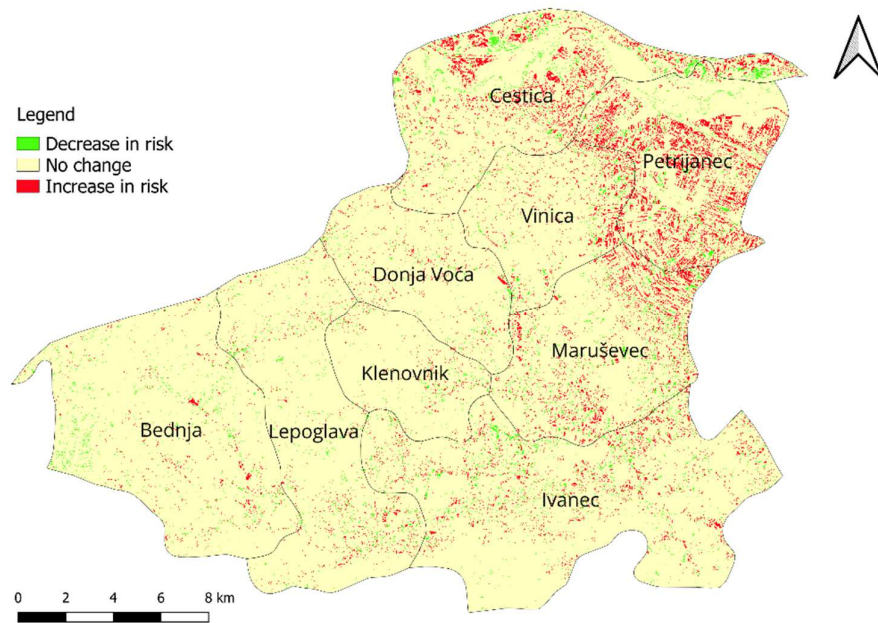


**Figure 15.** Landslide risk map in 2025 compared to 2024

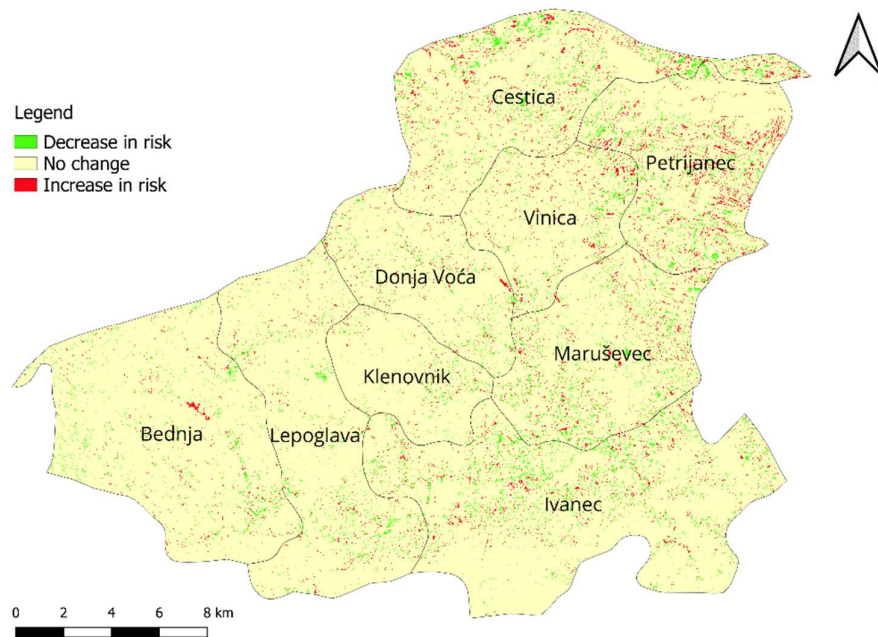


**Figure 16.** Landslide risk map in 2025 compared to 2023

#### 4. DISCUSSION

The landslide risk analysis for nine municipalities in Varaždin County shows results that are in agreement with the relief and known conditions of the area. Municipalities in the hilly part (Donja Voća, Klenovnik, Bednja, Lepoglava, Ivanec) have the largest share of high and very high-risk category, while flat areas along the Drava River (Cestica, Petrijanec, Maruševec) are mostly in the low or very low categories. For example, in 2023 the high-risk (category 4) covered 14.05% or 69.59 km<sup>2</sup>, while the very high (category 5) was only 0.94% or 4.66 km<sup>2</sup>. In contrast, the share of very low risk (category 1) in the lowland municipalities reached more than 8% in 2024 (39.90 km<sup>2</sup>), highlighting the clear difference between mountainous and flat terrain. This is in line with earlier national studies, which also pointed out northwestern Croatia as one of the most unstable regions (Mihalić Arbanas et al. 2019).

**Table 12.** Changes in area and percentage by landslide risk categories

Risk Category	2024 vs 2023 [km <sup>2</sup> ]	2024 vs 2023 [%]	2025 vs 2024 [km <sup>2</sup> ]	2025 vs 2024 [%]	2025 vs 2023 [km <sup>2</sup> ]	2025 vs 2023 [%]
<b>1 – Decrease in risk</b>	28.75	5.81	11.20	2.26	17.44	3.52
<b>2 - No change</b>	457.64	92.42	458.97	92.69	466.49	94.21
<b>3 – Increase in risk</b>	8.79	1.76	25.01	5.05	11.25	2.27

#### 4.1. Temporal differences 2023–2025

Between the three years only small differences are visible. Very high risk covered 0.94% (4.66 km<sup>2</sup>) in 2023, 0.93% (4.58 km<sup>2</sup>) in 2024 and 0.92% (4.55 km<sup>2</sup>) in 2025. High risk decreased from 14.05% (69.59 km<sup>2</sup>) in 2023 to 13.32% (65.97 km<sup>2</sup>) in 2024, and then slightly increased again to 13.72% (67.96 km<sup>2</sup>) in 2025. At the same time, very low risk increased from 6.28% (31.12 km<sup>2</sup>) in 2023 to 8.06% (39.90 km<sup>2</sup>) in 2024, before it was again lower in 2025 with 6.60% (32.67 km<sup>2</sup>). This shows that 2024 was the most stable year, 2023 the least stable, while 2025 was in between.

The risk change maps confirm these numbers. Between 2023 and 2024, 28.75 km<sup>2</sup> (5.81%) of the area moved to lower risk and 8.79 km<sup>2</sup> (1.76%) to higher. Between 2024 and 2025, the situation was opposite: 25.01 km<sup>2</sup> (5.05%) moved to higher categories and 11.20 km<sup>2</sup> (2.26%) to lower. If we compare 2025 with 2023, again more decrease is visible (17.44 km<sup>2</sup>, 3.52%) than increase (11.25 km<sup>2</sup>, 2.27%).

When viewed across the entire study area, these changes are minimal. In all comparisons, less than 6% of the territory shifted from one risk category to another. Such limited changes point to minor local adjustments rather than to any broader alteration in the regional pattern of landslide risk.

#### 4.2. Explanation of results

The limited temporal variability mainly comes from the structure of the model. NDVI was the only dynamic factor with weight 20%, while slope (40%), aspect (25%) and land use (15%) are static and have stronger impact on the results. Because of this, the risk maps are mostly stable, since topography does not change in short time. The 10 m resolution of Sentinel-2 images also makes vegetation more uniform, so NDVI changes are not fully visible.

Still, some differences can be noticed. The higher share of very low risk in 2024 is connected with higher NDVI values in that year, which means denser and healthier vegetation. Stronger vegetation cover stabilises surface soil, reduces runoff and helps to protect slopes. In 2025 the NDVI values were lower, so the very low category was reduced again, showing that less vegetation makes slopes a little more unstable. These results agree with earlier studies where vegetation was seen as important protective factor for shallow landslides.

However, the influence of NDVI is small compared to slope and aspect. Changes like the decrease of very low risk from 39.90 km<sup>2</sup> in 2024 to 32.67 km<sup>2</sup> in 2025 are minor compared to the stable effect of relief. This shows that NDVI can explain small year-to-year variations, but the main pattern of risk is controlled by topography. For regional scale maps, vegetation dynamics can add useful information, but they cannot change the dominant role of geomorphology.

#### 4.3. Limitations

The main limitation of this study is that lithology was not included. Previous research showed that Neogene and Quaternary clays and marls are the key reason for many landslides in northwestern Croatia. Without geological data, some areas that appear stable on the maps may in reality be prone to slope movements, while some areas classified as unstable may not have real hazard. In addition, precipitation, soil moisture and groundwater were also not considered, although they are important triggers for landslides.

Because of these missing factors, the produced maps should be understood as first approximation on regional level. They can show general spatial patterns and help in awareness and planning, but they cannot give precise prediction of where landslides will occur.

## 5. CONCLUSIONS

Within this study, a landslide risk map was created for nine municipalities of Varaždin County using open-access datasets and QGIS software. The analysis revealed a pronounced contrast between the hilly municipalities, which show higher risk, and the lowland municipalities along the Drava River, where risk is generally low. These results demonstrate that even with a relatively simple approach, open data and free GIS tools can provide a reliable basis for regional-scale risk assessment and support spatial planning and hazard management.

Differences between years are very small, which shows that results are stable and mainly follow geomorphological conditions. Maps can therefore be used as first orientation for awareness of landslide hazard and for needs of spatial planning. Use of open data and free software proved to be practical and efficient, so this type of approach can be applied also in other parts of Croatia and in similar regions.

The study also shows that a relatively simple methodology can still give meaningful results if it is carefully applied to local conditions. Even though some important factors were not included, the produced maps give a useful overview which can help in decision making and in prioritising areas for detailed field investigations.

For future research it is recommended to integrate geological and hydrological data, to test alternative weighting schemes, and to validate results with detailed landslide inventories. This would improve the reliability of the model and provide stronger support for local authorities. In the long term, such studies can contribute to reducing remediation costs and increasing the safety of local communities.

## 6. REFERENCES

Ayalew L, Yamagishi H (2025) The application of GIS-based logistic regression for landslide susceptibility mapping in the Kakuda-Yahiko Mountains, Central Japan. *Geomorphology*, 65, 15–31. doi: [10.1016/j.geomorph.2004.06.010](https://doi.org/10.1016/j.geomorph.2004.06.010).

Copernicus Data Space Ecosystem. Sentinel-2 Data Overview: Multispectral imagery for land monitoring. Available at <https://dataspace.copernicus.eu/explore-data/data-collections/sentinel-data/sentinel-2>. Cited 15 July 2025.

Copernicus Land Monitoring Service. CLCplus Backbone 2023: 10 m Raster Land Cover/Land Use Classification Based on Sentinel-2 Time Series, 11-Class Nomenclature, Reference Year 2023. European Environment Agency, 2025. Available at <https://land.copernicus.eu/en/products/clc-backbone>. Cited 5 July 2025.

Corominas J, van Westen C, Frattini P, Cascini L, Malet J P (2014) Fotopoulou, S.; Catani, F. Recommendations for the quantitative analysis of landslide risk. *Bull. Eng. Geol. Environ.* 73, 209–263. doi: [10.1007/s10064-013-0538-8](https://doi.org/10.1007/s10064-013-0538-8).

Cruden D M, Varnes D J (1996) Landslide Types and Processes. In *Landslides: Investigation and Mitigation*; Turner, A.K., Schuster, R.L., Eds.; Transportation Research Board, National Academy Press: Washington, DC, USA, pp. 36–75.

DIVA-GIS. Select and download free geographic (GIS) data for any country in the world. Administrative areas. Available at <https://diva-gis.org/data.html>. Cited 23 June 2025.

ESA. Copernicus Digital Elevation Model (DEM) – GLO-30. European Space Agency, 2020. Available at <https://dataspace.copernicus.eu/>. Cited 28 June 2025).

Esri. How Slope Works – ArcGIS Pro Documentation. 2024. Available at <https://pro.arcgis.com/en/pro-app/latest/tool-reference/spatial-analyst/how-slope-works.htm>. Cited 2 August 2025.

European Space Agency. Sentinel 2 Mission Overview: 13 spectral bands for land and vegetation monitoring. Copernicus Data Space Ecosystem, 2025. Available at <https://dataspace.copernicus.eu>. Cited 14 July 2025.

Fuad N, Meandad J, Haque, A, Sultana, R, Anwar S B, Sultana S (2024) Landslide vulnerability analysis using frequency ratio (FR) model: a study on Bandarban district, Bangladesh. *arXiv*, arXiv:2407.20239. doi: [10.48550/arXiv.2407.20239](https://doi.org/10.48550/arXiv.2407.20239).

Gazibara B, Novak M, Ivanec T, Vrbanec A (2023) Landslide Susceptibility Assessment on a Large Scale in the City of Zagreb (Croatia). *Geomatics, Natural Hazards and Risk*, 14(1), 239–263. doi: [10.1080/17445647.2022.2163197](https://doi.org/10.1080/17445647.2022.2163197).

Guth P L, Van Niekerk, A, Grohmann C H, et al (2021) Digital Elevation Models: Terminology and Definitions. *Remote Sensing*, 13(18), 3581. doi: [10.3390/rs13183581](https://doi.org/10.3390/rs13183581).

Guzzetti F, Carrara A, Cardinali M, Reichenbach P (1999) Landslide hazard evaluation: a review of current techniques and their application in a multi-scale study, Central Italy. *Geomorphology* 1999, 31, 181–216. doi: [10.1016/S0169-555X\(99\)00078-1](https://doi.org/10.1016/S0169-555X(99)00078-1)

He Q, Wu S, Zhao, X, Hui Z, Wang Z (2025) Tsangaratos, P.; Ilija, I.; Chen, W.; Chen, Y.; Hao, Y. Evaluation of landslide susceptibility of mountain highway based on RF and SVM models. *Sci. Rep.* 15, 24991. doi: [10.1038/s41598-025-08774-w](https://doi.org/10.1038/s41598-025-08774-w).

Horn B K P Hill (1981) Shading and the Reflectance Map. *Proc. IEEE*. 69(1), 14–47. doi: [10.1109/PROC.1981.11918](https://doi.org/10.1109/PROC.1981.11918).

Hung O, Leroueil S, Picarelli L (2014) The Varnes classification of landslide types, an update. *Landslides*, 11, 167–194. doi: [10.1007/s10346-013-0436-y](https://doi.org/10.1007/s10346-013-0436-y).

- Issaoui W, Nas I H, Alexakis D D, Bejaoui W, Ibraheem I M, Ezzine A, Ben Othman D, Inoubli M H (2024) Geometric Characterization of the Mateur Plain in Northern Tunisia Using Vertical Electrical Sounding and Remote Sensing Techniques. *ISPRS Int. J. Geo-Inf.* 13(9), 333. doi: <https://doi.org/10.3390/ijgi13090333>.
- Jug J, Grabar K, Bek A, Strelec S (2024) Stabilization of Shallow Landslides Induced by Rainwater Infiltration—A Case Study from Northern Croatia. *Geotechnics*. 4(1), 242–263. doi: [10.3390/geotechnics4010013](https://doi.org/10.3390/geotechnics4010013).
- Klimeš J, Rios Escobar V (2010) A Landslide Susceptibility Assessment in Urban Areas Based on Existing Data: An Example from the Iguañá Valley, Medellín City, Colombia. *Nat. Hazards Earth Syst. Sci.* 10, 2067–2079. doi: [10.5194/nhess-10-2067-2010](https://doi.org/10.5194/nhess-10-2067-2010).
- Lapaine M (2024) 20th Anniversary of the New Official Map Projections in Croatia. *Geodetski list* 78 (101), no. 1. 31–44. Available at <https://hrcak.srce.hr/317490>.
- Liu X, Shao S, Shao S (2024) Landslide susceptibility zonation using the analytical hierarchy process (AHP) in the Great Xi'an Region, China. *Sci. Rep.* 14, 53630. doi: [10.1038/s41598-024-53630-y](https://doi.org/10.1038/s41598-024-53630-y).
- Malczewski J (1999) *GIS and Multicriteria Decision Analysis*; Wiley: New York, NY, USA.
- Mersha T, Meten, M (2020) GIS-based landslide susceptibility mapping using logistic regression analysis in Debre Sina area, Ethiopia. *Geoenviron. Disasters*, 7, 20. doi: [10.1186/s40677-020-00155-x](https://doi.org/10.1186/s40677-020-00155-x)
- Mihalić Arbanas S, Bernat Gazibara S, Krkač M, Arbanas Ž (2017) Landslides in the Dinarides and Pannonian Basin—From the Largest Historical and Recent Landslides in Croatia to Catastrophic Landslides Caused by Cyclone Tamara. *Landslides* 2017, 14, 1861–1876. doi: [10.1007/s10346-017-0880-1](https://doi.org/10.1007/s10346-017-0880-1)
- Mihalić Arbanas S, Bernat Gazibara S, Krkač M, Sečanj M (2019) *Studija: Procjena podložnosti na klizanje Republike Hrvatske; Rudarsko-geološko-naftni fakultet, Sveučilište u Zagrebu*; Zagreb, Croatia.
- Monopoli R, et al (2024) Landslide Mapping from Sentinel-2 Imagery Through Change Detection. *arXiv*, arXiv:2405.20161. doi: [10.48550/arXiv.2405.20161](https://doi.org/10.48550/arXiv.2405.20161).
- Nedd R (2021) Land-Use and Land-Cover: Definitions, Usage and Misuse. *Land* 10(9), 994. doi: [10.3390/land10090994](https://doi.org/10.3390/land10090994).
- Notti D, Cignetti M, Godone D, Giordan D (2023) Semi-automatic mapping of shallow landslides using free Sentinel-2 images and Google Earth Engine. *Nat. Hazards Earth Syst. Sci.* 23, 2625–2648. doi: [10.5194/nhess-23-2625-2023](https://doi.org/10.5194/nhess-23-2625-2023).
- O'Donohue, D Calculating NDVI Using QGIS. *MapScaping Blog*, 13 September 2023. Available at <https://mapscaping.com/calculating-ndvi-using-qgis>. Cited 18 August 2025.
- Plank S, Twele A, Martinis S (2016) Landslide Mapping in Vegetated Areas Using Change Detection Based on Optical and Polarimetric SAR Data. *Remote Sens.* 8, 307. doi: [10.3390/rs804030](https://doi.org/10.3390/rs804030).
- Podolszki L, Karlović I (2023) Remote Sensing and GIS in Landslide Management: A Case Study of Kravarsko, Croatia. *Remote Sens.* 15, 5519. doi: [10.3390/rs15235519](https://doi.org/10.3390/rs15235519).
- Pourghasemi H R, Pradhan B, Gokceoglu C, Moezzi K D (2012) Landslide susceptibility mapping using a spatial multi-criteria evaluation model at Haraz watershed, Iran. *Landslides*, 9, 511–526. doi: [10.1007/978-3-642-25495-6\\_2](https://doi.org/10.1007/978-3-642-25495-6_2).
- Putra A N, Jaenudin Prasetya N R, Sugiarto MT, et al (2025) Utilizing Remote Sensing and Random Forests to Identify Optimal Land Use Scenarios and Address the Increase in Landslide Susceptibility. *Sustainability*, 17, 4227. doi: [10.3390/su17094227](https://doi.org/10.3390/su17094227).
- QGIS Documentation Team. *QGIS Training Manual; QGIS Project: 2023*. Available at [https://docs.qgis.org/latest/en/docs/training\\_manual/](https://docs.qgis.org/latest/en/docs/training_manual/). Cited 16 August 2025.
- Rana H, Mushtaq T, Anburaj R (2025) Impact of geofactors on landslide susceptibility using weighted overlay method: An integrated GIS and field-based analysis on NH-07, Chamoli, Uttarakhand. *Geosystems and Geoenvironment*, 4, 100420. doi: [10.1016/j.geogeo.2025.100420](https://doi.org/10.1016/j.geogeo.2025.100420).
- Reichenbach P, Rossi M, Malamud B D, Mihir M, Guzzetti F (2018) A review of statistically-based landslide susceptibility models. *Earth-Sci. Rev.* 180, 60–91. doi: [10.1016/j.earscirev.2018.03.001](https://doi.org/10.1016/j.earscirev.2018.03.001).
- Sinčić M, Bernat Gazibara S, Krkač M, Mihalić Arbanas S (2022) Use of High-Resolution Remote Sensing Data in Landslide Hazard Assessment in Hrvatsko Zagorje. *Land*, 11, 1360. doi: [10.3390/land11081360](https://doi.org/10.3390/land11081360).
- Swain J B, Singh N J, Gupta L R. (2024) Landslide susceptibility zonation of a hilly region: A quantitative approach. *Nat. Hazards Res.* 4(1), 75–86. doi: [10.1016/j.nhres.2023.07.008](https://doi.org/10.1016/j.nhres.2023.07.008).
- Tzampoglou M, Floros G, Tsakiri K, Petropoulos G P (2025) A GIS-based landslide susceptibility mapping using ensemble learning techniques: A case study from Western Greece. *Geosciences*, 15(2). doi: [10.1016/j.sciaf.2025.e02661](https://doi.org/10.1016/j.sciaf.2025.e02661).
- Varaždinska županija. U Varaždinskoj županiji u tri godine sanirano čak 55 klizišta; štete od novih klizišta u svibnju 2023. dosegule 40,95 milijuna eura. Available via: <https://www.varazdinska-zupanija.hr/vijesti/u-varazdinskoj-zupaniji-u-tri-godine-sanirano-cak-55-klizista-tri-je-danas-obisao-potpredsjednik-vlade-i-ministar-bacic-sa-zupanom-stricakom.html>. Cited 20 August 2025.
- Varnes D J (1978) Slope Movement Types and Processes. In *Landslides: Analysis and Control*; Schuster, R.L., Krizek, R.J., Eds.; Transportation Research Board, National Academy of Sciences: Washington, DC, USA, pp. 11–33.
- Wang L, Wu B, Zhu W, Elnashar A, Yan N, Ma Z (2025) Evapotranspiration Disaggregation Using an Integrated Indicating Factor Based on Slope Units. *Remote Sens.* 17, 1201. doi: [10.3390/rs17071201](https://doi.org/10.3390/rs17071201)

Wen T H, Teo T A (2022) Landslide Inventory Mapping from Landsat-8 NDVI Time Series Using Adaptive Landslide Interval Detection. *ISPRS Annals of the Photogrammetry, Remote Sensing and Spatial Information Sciences*, V-3, 557–562. doi: [10.5194/isprs-annals-V-3-2022-557-2022](https://doi.org/10.5194/isprs-annals-V-3-2022-557-2022).

Xiong H, Zhu A X, Wang R, Zhou C, Liu J (2022) Geomorphometry and Terrain Analysis: Data, Methods, and Applications. *Earth-Science Reviews*, 232, 104120. doi: [10.1016/j.earscirev.2022.104191](https://doi.org/10.1016/j.earscirev.2022.104191).

Zhang G, Liu Y, Chen Z et al (2025) Production and Analysis of a Landslide Susceptibility Map Covering Entire China. *Remote Sens.* 17, 1615. doi: [10.3390/rs17091615](https://doi.org/10.3390/rs17091615).

Zhao Q, Yang H, Zhang Y, et al (2024) The Retrieval of Ground NDVI (Normalized Difference Vegetation Index). *Remote Sens.* 16, doi: [10.3390/rs16071212](https://doi.org/10.3390/rs16071212)

Zhu, Y, Li H, Tang R et al (2025) Assessing the Influence of Environmental Factors on Landslide Frequency and Intensity in Northwestern Sichuan, SW China, Using Multi-Temporal Satellite Imagery. *Remote Sens.* 17, 2083. doi: [10.3390/rs17122083](https://doi.org/10.3390/rs17122083).